Dexamethasone-Induced Oxidative Stress Enhances Myeloma Cell Radiosensitization While Sparing Normal Bone Marrow Hematopoiesis[1]

Soumen Bera*, Suzanne Greiner[†], Amit Choudhury[‡], Angela Dispenzieri[§], Douglas R. Spitz*, Stephen J. Russell[†] and Apollina Goel*

*Free Radical and Radiation Biology Program, Department of Radiation Oncology, The Holden Comprehensive Cancer Center, University of Iowa, Iowa City, IA, USA; [†]Molecular Medicine Program, Rochester, MN, USA; [‡]Department of Anatomy and Cell Biology, The Holden Comprehensive Cancer Center, University of Iowa, Iowa City, IA, USA; [§]Mayo Clinic College of Medicine, Rochester, MN, USA

Abstract

Dexamethasone (Dex) and radiation therapy are established modalities in multiple myeloma. In this study, we propose a novel combination of Dex plus radiation that shows superior clonogenic cell killing and apoptosis of myeloma cells and selectively eliminates myeloma cells when cocultured with bone marrow stromal cells (BMSCs). Dex was found to inhibit the release of interleukin-6 from irradiated BMSCs, which is an established myeloma cell proproliferative cytokine. In 5TGM1 model, the combination of Dex with skeletal targeted radiotherapy (153-Sm-EDTMP) prolonged median survival time and inhibited radiation-induced myelosuppression. A two-cycle treatment of Dex plus 153-Sm-EDTMP was well tolerated and further improved median survival time. Mechanistically, Dex increased superoxide and hydrogen peroxide production and augmented radiation-induced oxidative stress and cell death of myeloma cells. In contrast, Dex inhibited radiation-induced increase in pro-oxidant levels and enhanced the clonogenic survival in normal hematopoietic stem and progenitor cells. Treatment with either N-acetylcysteine or the combination of polyethylene glycol (PEG)–conjugated copper, zinc-superoxide dismutase, and PEG-catalase significantly protected myeloma cells from Dex-induced clonogenic death. Overall, these results demonstrate that Dex in combination with radiotherapy enhances the killing of myeloma cells while protecting normal bone marrow hematopoiesis through a mechanism that involves selective increases in oxidative stress.

Neoplasia (2010) 12, 980–992

Introduction

Radiation therapy is a powerful treatment modality for multiple myeloma (MM) [1,2]. External beam irradiation is frequently used for palliation of bone pain and eradication of solitary plasmacytomas [3,4]. In myeloma patients who present diffused bone disease, systemic radiotherapy with agents such as bone-seeking radionuclides and radioimmunotherapy [5,6] or alternative techniques like intensity-modulated radiation therapy and helical tomography [7,8] have been explored. Bone-seeking radionuclide therapy with radioactive samarium conjugated to a tetraphosphonate chelator (153-Sm-EDTMP) has been used in myeloablative clinical protocols for MM [9–12]. The combination of radiotherapy with novel chemotherapeutic agents such as thalidomide [13] and bortezomib [14,15] has shown good clinical outcomes with reduced radiotoxicity to normal tissues. Testing of

antimyeloma drugs in combination with bone-seeking radiotherapy is worthy of investigation because MM is an inherently radiosensitive malignancy. Furthermore, such radiation-based combination regimens may require less aggressive interventions (nonmyeloablative) that could

be offered to elderly patients who comprise the present and future majority of MM patients [16,17].

Dexamethasone (Dex) is a synthetic steroidal glucocorticoid that is widely used in the treatment of MM in single [18] and combination chemotherapy regimens [19]. The antimyeloma effect of Dex has been partly elucidated [20,21]. The major impediments to the effective use of Dex in myeloma cure are acquired Dex resistance due to prolonged usage and/or disease progression [22,23] and toxicities with combination chemotherapy agents without an improved survival benefit [24]. Dex is also an anti-inflammatory drug that inhibits the activation of the redox-regulated prosurvival transcription factors nuclear factor κB (NF-κB) and activator protein 1 (AP-1) that govern cellular radiosensitivity [25]. Dex has been shown to inhibit IL-6 expression [26], and an NF-κB– and c-Jun–mediated IL-6 expression has been reported in myeloma cells [27]. IL-6 has been established as a prosurvival and proproliferative cytokine in MM [28] that may be regulated by the redox status of the tumor cells [29]. On the basis of the direct myeloma cytotoxicity and anti-inflammatory nature of Dex, we hypothesized that Dex-induced redox perturbations could potentially augment radiation-induced myeloma cell death by enhancing oxidative stress.

Myeloma cells may exist in a pro-oxidant state as evidenced by increased markers of lipid peroxidation and lower levels of antioxidant enzymes in patients with MM, relative to healthy controls [30–32]. Dex has been suggested to induce oxidative cell death in T-cell lymphoma [33–35]; however, a clear role for Dex in inducing oxidative stress in MM has not been established [36,37]. In normal cells, Dex has been shown to inhibit reactive oxygen species (ROS) generation in mononuclear cells and polymorphonuclear leukocytes [38], protect hepatocytes against cadmium toxicity by increasing levels of metallothionein and cellular thiols [39] and reduce oxidative DNA fragmentation induced by hydrogen peroxide (H_2O_2) in the nasal mucosa [40]. It is well established that ionizing radiation (IR) actuates the production of free radicals (such as superoxide [$O_2^{\bullet-}$] and H_2O_2) that induce oxidative stress–induced cell death [25]. Because myeloma cells seem to demonstrate increased levels of endogenous metabolic oxidative stress, relative to normal cells, and radiation is a potent exogenous inducer of oxidative stress, we hypothesized that combining radiation with Dex would selectively augment the killing of myeloma cells relative to bone marrow (BM)–resident cells.

This study shows that Dex can be effectively combined with radiation to improve therapeutic efficacy in MM. Mechanistically, Dex selectively induces oxidative stress–induced cell killing in myeloma cells compared with BM stromal cells and hematopoietic stem/progenitor cells. This study provides a new paradigm for Dex usage in MM that can potentially be incorporated in designing more effective combined modality therapies.

Materials and Methods

Cell Culture

Cell lines were obtained from the American Type Culture Collection (RPMI 8226 [CCL-155], SR-4987 [CRL-2028], and HS-5 [CRL-11882]; ATCC, Manassas, VA) or were kind gifts from Dr Steven Rosen (MM.1S and MM.1R; Northwestern University, Chicago, IL), Dr Greg Mundy (5TGM1; University of Texas Health Science Center at San Antonio, TX), Dr Toshiyuki Yoneda (5TGM1-Luc; University of Texas Health Science Center at San Antonio, TX), or Dr Diane Jelinek (KAS-6/1 and ANBL-6; Mayo Clinic, Rochester, MN). 5TGM1 cells

stably expressing emerald fluorescent protein (eFP) along with firefly luciferase (Luc) protein (5TGM1-eFP-Luc) was generated using a viral vector harboring the eFP and Luc transgene under control of the spleen focus–forming virus U3 promoter with an internal ribosome entry site. Similarly, SR-4987 cells stably expressing red fluorescent protein (SR-4987-DsRed) were established. All cell lines were grown in RPMI 1640 medium (Gibco, Invitrogen, Carlsbad, CA) supplemented with 10% fetal bovine serum (Gibco), 100 U/ml penicillin (Gibco), 100 mg/ml streptomycin (Gibco), and 50 μM β-mercaptoethanol (referred to as complete medium) in a humidity-controlled incubator (37°C and 5% CO_2).

The normal hematopoietic stem cells (HSCs) and hematopoietic progenitor cells (HPCs) were isolated from C57BL/6 mice (8-10 weeks old) that were purchased from The Jackson Laboratory (Bar Harbor, ME) and housed at The University of Iowa Animal Care Facility. The Institutional Animal Care and Use Committee approved the animal procedures used in this study. Briefly, BM was collected from mice (n = 10 per experiment), and a lineage-negative (Lin$^-$) cell population was isolated (Stem Cell Technologies, Inc). Cells were separated into HPCs (Lin$^-$c-kit$^+$Sca1$^-$ or LKS$^-$ cells) and HSCs (Lin$^-$c-kit$^+$Sca1$^+$ or LKS$^+$ cells) LKS$^+$ population [41].

Propidium Iodide Uptake

The percentage of dead cells was determined by a propidium iodide (PI) uptake assay. Cells (2.5×10^4 for myeloma cells and 0.5×10^4 for BMSCs) were seeded in 96-well flat-bottom plates, in a phenol red–free RPMI 1640 (Gibco) complete medium. Triplicate wells were treated with 0, 1, or 5 μM Dex (Sigma-Aldrich, St Louis, MO) for 24 or 48 hours and then left untreated or subjected to radiation treatment (6 Gy). All irradiations were performed at the Radiation and Free Radical Core Facility (The University of Iowa Holden Comprehensive Cancer Center), using a cesium-137 γ radiation source at a dose rate of 0.83 Gy/min. At 24 hours after radiation, PI (Sigma-Aldrich) was added (1 μg/ml in PBS), plates were incubated for 60 minutes at 37°C, and fluorescence was measured (Infinite M200; Tecan, Research Triangle Park, NC; λ_{ex} = 530 nm, λ_{em} = 645 nm). The percentage of dead cells was calculated as the proportion of fluorescence intensity relative to that in the untreated control (the latter being set at 100% viability).

Clonogenic Assays

The colony-forming ability of cell lines and primary cells was determined as described before with minor modifications [42]. Cells were treated without or with Dex (5 μM for 12 hours) and then left untreated or given radiation (6 Gy). In specific experiments, the glutathione precursor N-acetylcysteine (NAC, 10 mM; Sigma-Aldrich) was added 1 hour before Dex. After various treatments, cells were moved to ice and plated (in triplicate) in basic methylcellulose medium (Stem Cell Technologies Inc, Vancouver, British Columbia, Canada) for myeloma cells or complete medium for BMSCs. The plating efficiency of cell lines was calculated by the following formula: PE = (number of colonies counted/number of cells seeded) × 100. Survival fractions were calculated as follows: (number of colonies counted)/(number of cells seeded × PE). For each cell population, the normalized survival fraction (NSF), relative to the number of untreated control cells, was calculated. The plating efficiencies of ANBL-6, 5TGM1, HS-5, and SR-4987 were 30, 28, 20, and 27.2, respectively.

For analyzing the colony-forming ability of HPCs or HSCs, cells were treated without or with Dex (5 μM for 6 hours) followed by mock or 6 Gy of radiation. Cells were plated in methylcellulose medium containing recombinant cytokines and erythropoietin (Stem

Cell Technologies, Inc). Plates were incubated at 37°C for 6 days and PE (12 and 8 hours for HSCs and HPCs, respectively), and the NSF was calculated.

JC-1 Staining

Loss of mitochondrial membrane potential was measured using the MitoProbe JC-1 assay (Molecular Probes, Invitrogen). The seeding density and medium for myeloma and BMSCs was similar to the PI assay followed by treatment with Dex (5 μM for 24 hours) and/or radiation (6 Gy). Cells were treated with the proton ionophore carbonyl cyanide 3-chlorophenylhydrazone (50 μM) to obtain positive controls. Six hours after radiation, the cells were incubated with JC-1 (200 nM) at 37°C for 30 minutes in the dark and were read using a plate reader (Tecan; λ_{ex} = 485 nm, λ_{em} = 595 nm for red fluorescence and λ_{ex} = 485 nm, λ_{em} = 535 nm for green fluorescence). For each sample, the average of triplicate samples was taken, and the ratio of red/green fluorescence intensity was calculated.

Caspase-3 Activity Assay

Apoptosis was measured using a caspase-3 fluorescence assay (Cayman Chemical Company, Ann Arbor, MI). Myeloma cells (1.0×10^4 cells/well) or BMSCs (0.2×10^4 cells/well) were seeded in 96-well plates in complete medium in triplicate and then treated with Dex (5 μM for 24 hours) and/or radiation (6 Gy). Lysates were collected 12 hours after radiation (without or with caspase-3 inhibitor N-Ac-Asp-Glu-Val-Asp-CHO) and used to measure caspase-3 activity (Tecan; λ_{ex} = 485 nm, λ_{em} = 535 nm). Caspase-3 activity was calculated and expressed as units per milligram of total protein.

Western Blot Analysis

Myeloma cells were treated with Dex (5 μM for 24 hours) and/or radiation (6 Gy), and total cell lysates were prepared 24 hours after radiation, using lysis buffer (Santa Cruz Biotechnology Inc, Santa Cruz, CA) supplemented with a protease-inhibitor cocktail. The anti–poly ADP-ribose polymerase (PARP) antibody with specificity toward both the full-length (113 kDa) and the cleaved large fragment of PARP (89 kDa) or α-tubulin (Cell Signaling Technology, Inc, Danvers, MA) antibody was used. Blots were developed using enhanced chemiluminescence (Pierce Biotechnology, Rockford, IL). Densitometric analyses for protein quantification were carried out using Image J 1.38x software (http://rsbweb.nih.gov/ij/index.html).

In Vitro Coculture Studies

Cocultures of 5TGM1-eFP-Luc MM cells and BMSCs (SR-4987 or SR-4987-DsRed) were established. Briefly, BMSCs were plated in complete medium in 96-well plates (2×10^2 cells/well, in triplicate) and allowed to adhere for 12 hours. 5TGM1-eFP-Luc cells (2×10^3 cells/well) were then added alone (monoculture) or cocultured with the BMSCs for 24 hours. Wells were then either left unirradiated or exposed to 6 Gy of radiation. At 24 and 48 hours after radiation, a luciferase assay (Promega, Inc, Madison, WI) was performed, and results were compared with time 0. The fluorescence images of 5TGM1-eFP-Luc and SR-4987-DsRed in coculture were acquired using an inverted fluorescence microscope (Eclipse TS-100F; Nikon, Melville, NY [magnification, ×40]) with Chroma filter sets fluorescein isothiocyanate (λ_{ex} = 480, band-pass = 40 nm; λ_{em} = 535, band-pass = 40 nm) and Cy3 (λ_{ex} = 535, band-pass = 50 nm, λ_{em} = 610, band-pass = 75 nm), respectively.

ELISA

5TGM1 (5×10^5 cells/well) or SR-4987 cells (1×10^5 cells/well) were seeded in six-well plates in complete medium overnight. Cells were treated with Dex (5 μM for 24 hours) followed by radiation (6 Gy), and culture supernatants were collected 24 hours after radiation. Controls included no treatment, Dex alone, and radiation alone. IL-6 levels in the supernatant were measured using a commercially available ELISA kit (eBiosciences, San Diego, CA).

3-(4, 5-Dimethylthiazolyl-2)-2, 5-diphenyltetrazolium Bromide Assay

The proliferative support of conditioned supernatant obtained from SR-4987 cells (CM) or SR-4987 cells exposed to 6-Gy radiation treatment (irradiated cell conditioned medium [ICCM] 24 hours after radiation) or exogenous IL-6 (50 ng/ml; R&D Systems, Minneapolis, MN) was determined by 3-(4, 5-dimethylthiazolyl-2)-2, 5-diphenyltetrazolium bromide (MTT) assay (ATCC) as described before [43]. 5TGM1 cells (1×10^4 cells/well in a 96-well plate) were seeded in triplicates using CM, ICCM, or IL-6 supplemented medium. At 48 hours, MTT assay was performed, and absorbance was read at 570 nm (Tecan). The relative proliferation at 48 hours for untreated control was set to 1, and the fold change with treatments was calculated.

In Vivo Therapy Studies

Experiments with 153-Sm-EDTMP (imaging and survival studies) were carried out at the Mayo Clinic, Rochester, MN, in accordance with the guidelines of the Mayo Clinic Animal Use and Care Committee. 153-Sm-EDTMP was provided by Cytogen Corporation (Princeton, NJ). A syngeneic, orthotopic mouse model of 5TGM1-Luc myeloma in C57BL/KaLwRij mice (Harlan CPB, Horst, The Netherlands) was used as described by us previously [42,44]. In vivo treatments were started on day 12 after tumor implantation, with the cohorts ($n = 6$ mice/group) treated with 1) phosphate buffered saline (PBS), days 12 to 16; 2) Dex (Dex phosphate; American Pharmaceutical Partners, Inc, Schaumburg, IL) at 1 mg/kg body weight, days 12 to 16; 3) 153-Sm-EDTMP at 22.5 MBq, day 13; or 4) Dex plus 153-Sm-EDTMP. Both Dex and 153-Sm-EDTMP were injected intraperitoneally. Complete blood cell counts were carried out on days 12 (baseline count), 18, and 21 after tumor cell inoculation, using a blood analyzer (VetScan HM II; Abaxis, Union City, CA) at the Toxicology and Pharmacology Laboratory (Mayo Clinic). In addition, tumor burden was evaluated in a noninvasive manner, on days 18 and 24 after tumor cell injection, using the IVIS 200 Bioluminescence Imaging System (Xenogen Corp, Hopkinton, MA). In the repeat dosing regimen, the first cycle of treatment was initiated on day 12 (as in the one-cycle regimen) followed by a second cycle of treatment initiated on day 22, where Dex was given on days 22 to 26 and 153-Sm-EDTMP was given on day 23. For survival studies, mice were followed until they reached the humane end point.

Measurements of Intracellular Superoxide ($O_2^{\bullet-}$) Levels

Steady-state levels of $O_2^{\bullet-}$ were estimated using the fluorescent dye, dihydroethidium (DHE; Molecular Probes, Invitrogen). 5TGM1 (2.5×10^4/well) or SR-4987 cells (5×10^3/well) were seeded in 96-well plates (in triplicate) in phenol red–free complete medium. After 12 hours, cells were treated with Dex (5 μM for 24 hours), followed by no treatment or radiation (6 Gy), and then cultured for 6 hours. Dye labeling was done at 37°C for 30 minutes in PBS (containing 5 mM pyruvate) with DHE (10 μM; in 0.1% DMSO). To confirm that increases in DHE oxidation were indicative of changes in intracellular $O_2^{\bullet-}$, specific

wells were pretreated with PEG-SOD (100 U/ml for 1 hour) before and during DHE labeling. DHE oxidation was measured at λ_{ex} = 488 nm and λ_{em} = 650 nm (Tecan).

Measurements of Steady-State Levels of Intracellular Pro-oxidants

Pro-oxidant levels (presumably intracellular peroxides) were monitored using 5-(and-6)-carboxy-2′,7′-dichlorodihydrofluorescein diacetate (carboxy-H₂DCF-DA; Molecular Probes, Invitrogen) oxidation. Cells were seeded in 96-well plates similar to DHE protocol and treated with Dex (5 µM), preloaded with carboxy-H₂DCF-DA (10 µg/ml for 30 minutes) followed by radiation (6 Gy). The fluorescence of the oxidized probe was measured at 6 hours after radiation (Tecan; λ_{ex} = 495 nm, λ_{em} = 530 nm). To ascertain if H₂DCF-DA oxidation was due to H_2O_2, specific wells were pretreated with 100 U/ml PEG-catalase for 1 hour before the addition of Dex. For the positive control, cells were treated with H_2O_2 (100 nM for 1 hour) before the probe was added. For experiments with HSCs and HPCs, the cells were seeded overnight in 96-well plates (1.0×10^4/well, in triplicate). Dex and radiation treatments were similar to treatment of cell lines as described above. Specific wells were pretreated with NAC (10 mM for 1 hour) before the addition of Dex followed by irradiation and H₂DCF-DA oxidation was measured using a plate reader.

Statistical Analysis

GraphPad Prism 4.0 software (GraphPad Software, San Diego, CA) was used for data handling, analysis, and presentation. Statistical significance was determined using two-tailed unpaired t test with a confidence interval of 95%. Survival curves were generated using the Kaplan-Meier method, and the log-rank test was used to examine the significance of differences in survival between the groups.

Results

Dexamethasone Increases IR-induced Myeloma Cell Death In Vitro

In a panel of myeloma cells, we first assessed the cytotoxicity of Dex (1 µM) at both 24 and 48 hours after treatment. Both human (MM.1S, 8226, KAS-6/1, and ANBL-6) and a murine myeloma cell line (5TGM1) showed sensitivity to Dex-induced toxicity with a time-dependent increase in cell death (Figure 1A). Next, Dex (5 µM for 24 hours) was combined with radiation, and cell death was assessed at 24 hours after radiation treatment. Dex treatment induced myeloma cell killing with drug sensitivity similar to that observed in Figure 1A and radiation alone did not result in immediate cell death of myeloma cells. However, pretreatment with Dex significantly increased PI staining in all myeloma cell lines after radiation treatment. The results of Figure 1B support the hypothesis that Dex may be acting as a radiosensitizing drug in myeloma cell lines.

Clonogenic cell survival assays were performed to confirm the ability of Dex to sensitize myeloma cell lines to radiation treatment (Figure 1C). Treatment with Dex resulted in approximately 50% to 60% clonogenic reduction for myeloma cells and radiation alone caused approximately 60% and 30% reduction in the clonogenicity of ANBL-6 and 5TGM1 cells, respectively. When myeloma cells were pretreated with Dex followed by radiation treatment, the radiosensitization effect of Dex was clearly evident with a greater than 90% reduction in the colony-forming ability of cells compared with untreated controls. To determine whether Dex-mediated radiosensitization was

specific to myeloma cells and not to other cellular components of BM, clonogenic assays were performed in two well-established human- and mouse-immortalized BMSCs: HS-5 [45] and SR-4987 [46] (Figure 1C). BMSCs were found to be relatively resistant to Dex treatment, whereas exposure to 6 Gy of radiation resulted in an approximately 40% decrease in colony-forming ability of both stromal lines. However, pretreatment with Dex did not result in increased clonogenic cell death of BMSCs when Dex plus radiation treatment was used compared with radiation alone. Reverse transcription–polymerase chain reaction was used to confirm the presence of the functional glucocorticoid receptor α (GRα) isoform in all myeloma and stromal cells used in this study (data not shown). Together, the results presented in Figure 1 demonstrate that Dex is selectively cytotoxic to myeloma cells and can selectively sensitize myeloma cells to radiation treatment.

Dex Plus Radiation Treatment Results in Mitochondrial Dysfunction and Apoptotic Cell Death of Myeloma Cells

We next determined whether treatment with Dex and/or radiation induces loss in mitochondrial membrane potential ($\Delta\psi_m$) in myeloma cells (Figure 2A). In myeloma cells, both Dex or radiation treatment decreased the red/green JC-1 fluorescence ratio, indicative of mitochondrial depolarization. When cells were pretreated with Dex followed by radiation, a more profound decrease in $\Delta\psi_m$ was noted in myeloma cells than that observed after radiation treatment alone. Studies were extended to BMSCs where Dex pretreatment did not result in a further decrease in radiation-induced changes in $\Delta\psi_m$ (Figure 2A). Overall, the JC-1 results suggest that combined treatment of Dex plus radiation results in the depolarization of mitochondria that may be responsible for triggering mitochondrial transition pore opening and cell death seen by PI staining in Figure 1.

To determine whether $\Delta\psi_m$ changes result in the activation of caspase-3, myeloma cells were treated with Dex and/or radiation, and total caspase-3 activity was measured. For MM.1S cells, a significant increase in caspase-3 activity was detected after treatment with Dex or radiation, and this was further increased by the combination treatment (Figure 2B). Similarly for 5TGM1 cells, combined treatment of Dex plus radiation led to a significant increase in caspase-3 activity over that observed with Dex or radiation alone. Furthermore, in BMSCs, the combined treatment of Dex plus radiation did not lead to a further increase in caspase-3 activity over that seen with radiation alone. The role of caspase-3 activation in myeloma cell apoptosis was confirmed by measurement of the cleavage of PARP. With combination treatment, PARP cleavage was apparent in all myeloma cells (Figure 2C). Collectively, the data in Figure 2 support the hypothesis that myeloma cells treated with Dex plus radiation exhibit increased cell death over that produced by either agent alone and that this cell death may involve the mitochondrial pathway of apoptosis.

In Myeloma-BMSCs Cocultures, Dex Plus Radiation Treatment Selectively Kills Myeloma Cells and Inhibits Radiation-Induced IL-6 Production from BMSCs

To determine whether Dex plus radiation treatment is effective within the tumor microenvironment, studies were extended to a direct myeloma-BMSCs coculture model (Figure 3A). The in vitro proliferation of 5TGM1-Luc cells (5TGM1 cells expressing a luciferase marker) was accelerated when cocultured with SR-4987 BMSCs, relative to when grown as monocultures (Figure 3A). Treatment of cocultured myeloma cells (5TGM1-Luc and SR-4987) with Dex resulted in a marginal inhibition of myeloma cell proliferation, whereas radiation treatment
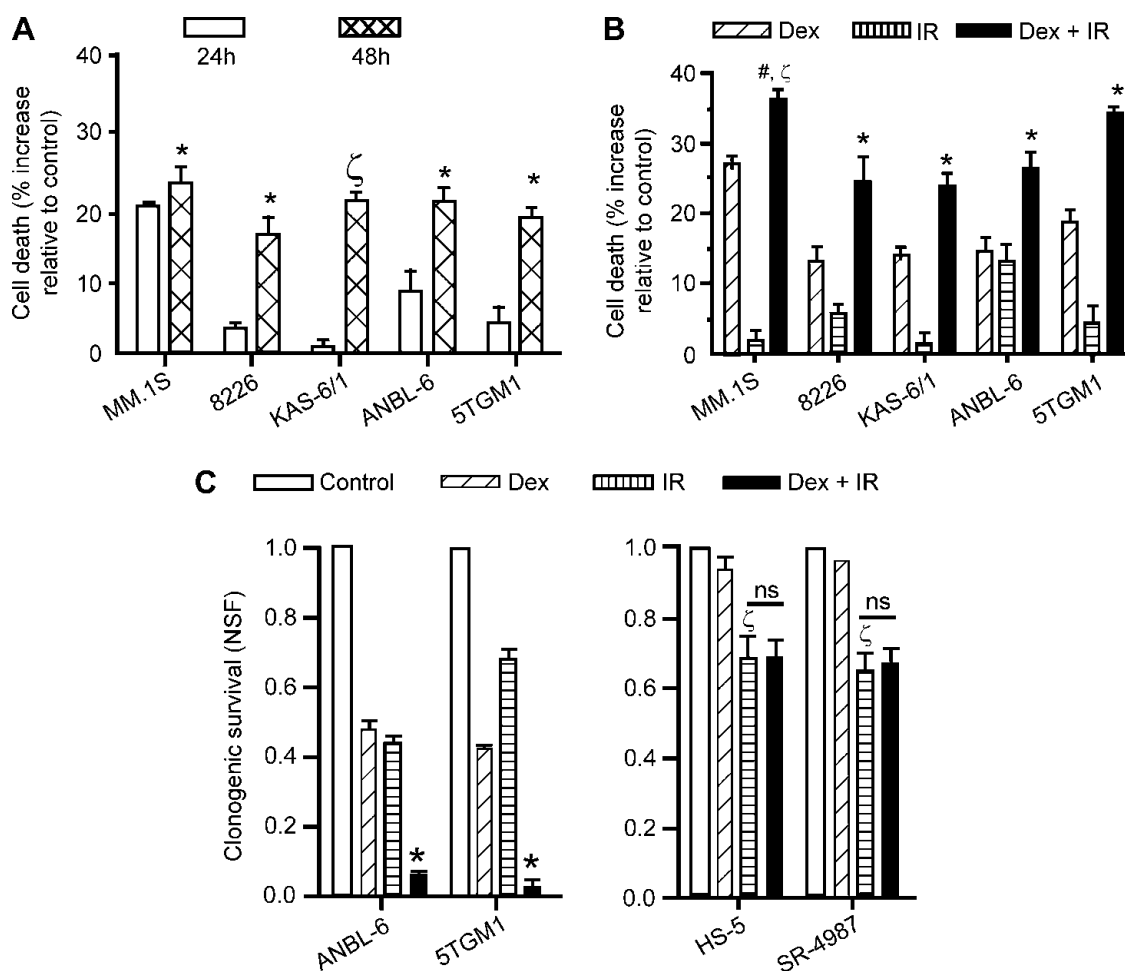
Figure 1. Dex induces myeloma cell cytotoxicity that is enhanced by radiation. Cell lines were treated with Dex and/or radiation, and cell death was determined by PI uptake (A, B) or clonogenic assay (C). (A) Myeloma cell cytotoxicity by Dex (1 μM) alone at 24 and 48 hours. *$P < .05$, $^{\zeta}P < .001$ *versus* 24 hours. (B) Myeloma cell cytotoxicity with treatment of Dex (5 μM) alone, radiation (6 Gy) alone, or Dex plus radiation at 24 hours. *$P < .05$ *versus* Dex or IR, $^{\zeta}P < .001$ *versus* IR, $^{\#}P < .05$ *versus* Dex. For panels A and B, results are mean of triplicate wells $\pm$ SD and representative of two independent experiments. The data are presented as percentage cell death relative to that in untreated controls. (C) NSF for myeloma (ANBL-6 or 5TGM1) and BMSCs (HS-5 or SR-4987) after Dex (5 μM) and/or 6 Gy of radiation. The results are representative of two independent experiments. *$P < .0005$ *versus* Dex or IR, $^{\zeta}P < .01$ *versus* control. ns indicates not significant. For panels A, B, and C, all statistical comparisons are with the respective cell types.

induced myeloma cell proliferation compared with untreated control cells. In contrast, Dex combined with radiation caused significant myeloma cell killing when compared with any other treatment group at 24 and 48 hours. To further assess the specificity of Dex plus radiation treatment, cocultures of eFP-expressing 5TGM1 cells and DsRed-expressing SR-4987 BMSCs were used. With Dex plus radiation treatment, it was apparent that only the 5TGM1 cells were being killed (Figure 3B). Results obtained from coculture studies (Figure 3, A and B) suggest that BMSCs are contributing, in a paracrine fashion, to acquired resistance to radiation in 5TGM1 cells and that the proposed combination treatment of Dex with radiation is effective in selectively eliminating the tumor cell population in cocultures.

Given that IL-6 has been established as a proproliferative cytokine for myeloma cells [47] and shown to be induced by radiation, we next determined whether irradiated myeloma cells or BMSCs was releasing IL-6 that may cause increased proliferation of myeloma cells seen in cocultures. In 5TGM1 cells, treatment with Dex or radiation inhibited IL-6 levels in the supernatant and Dex plus radiation treatment resulted in IL-6 concentrations lower than the untreated control (Figure 3C).

For SR-4987 cells, the basal concentration of IL-6 in untreated cells was 275.1 ± 20.4 pg/ml that was marginally inhibited by Dex treatment (233.9 ± 13.5 pg/ml; Figure 3C). With 6 Gy of radiation treatment, the IL-6 concentration in the SR-4987 culture supernatant increased to 627.5 ± 16.9 pg/ml. Notably, this radiation-induced IL-6 release by SR-4987 cells was completely blocked by Dex pretreatment, suggesting that irradiated BMSCs predominantly secrete IL-6 and that Dex can block the proproliferative effects of radiation in a coculture model system.

To determine whether exogenous IL-6 mimics the proproliferative effects of irradiated stromal cells, the ability of exogenous IL-6 and the culture medium obtained from irradiated BMSCs (ICCM) to stimulate myeloma cell proliferation was compared. Exogenous IL-6 resulted in increased 5TGM1 cell viability and proliferation (fold change of 1.3 ± 0.1) relative to tumor cells exposed to culture medium obtained from nonirradiated SR-4987 cells (Figure 3D). When myeloma cells were cultured in ICCM, a more pronounced increase in 5TGM1 proliferation was observed (1.7 ± 0.1), indicating that in addition to IL-6, other proinflammatory cytokines released by irradiated BMSCs may

be contributing to myeloma cell growth and proliferation. The presence of an IL-6 receptor complex in 5TGM1 cells was confirmed by Western blot analysis of whole cell lysates (data not shown). Overall, Figure 3 shows that with the Dex pretreatment, the release of IL-6 and other proinflammatory cytokines from irradiated BMSCs is attenuated, and this may be contributing to radiosensitization of myeloma cells in stromal cell cocultures.

Dex Enhances Skeletal Targeted Radiotherapy (153-Sm-EDTMP)-Mediated Tumor Suppression and Protects Peripheral Blood Cell Counts in the 5TGM1 Myeloma Model

To evaluate if Dex increases the cytotoxicity of radiation therapy *in vivo*, Dex was combined with 153-Sm-EDTMP in a systemic myeloma model. The response to therapy was measured by bioluminescence imaging (BLI) of 5TGM1-Luc cells (Table 1). On day 18 after radiation, the BLI signal was reduced by Dex or 153-Sm-EDTMP

treatments ($P < .005$ *vs* untreated control), which was further decreased with the combination treatment of Dex plus 153-Sm-EDTMP ($P < .0001$ *vs* untreated control). On day 24, average tumor growth in the group receiving Dex treatment alone was marginally lower compared with those in the control group ($P < .01$), indicating that Dex treatment alone may not be sufficient to inhibit tumor cell proliferation *in vivo*. Compared with Dex, 153-Sm-EDTMP exhibited a more pronounced inhibition of tumor growth ($P < .005$ *vs* control). In addition, combined treatment of Dex plus 153-Sm-EDTMP showed no tumor cell growth between days 18 and 24 ($P < .0001$ *vs* control). Furthermore, on day 24, the mean BLI units of Dex plus 153-Sm-EDTMP were significantly lower compared with the 153-Sm-EDTMP alone ($P < .0001$), thus showing Dex-enhanced tumor killing *in vivo*. Next, the median survival time of different treatment groups was compared (Figure 4A). The median survival of mice receiving no therapy was 26.5 days, and treatment with Dex or 153-Sm-EDTMP alone
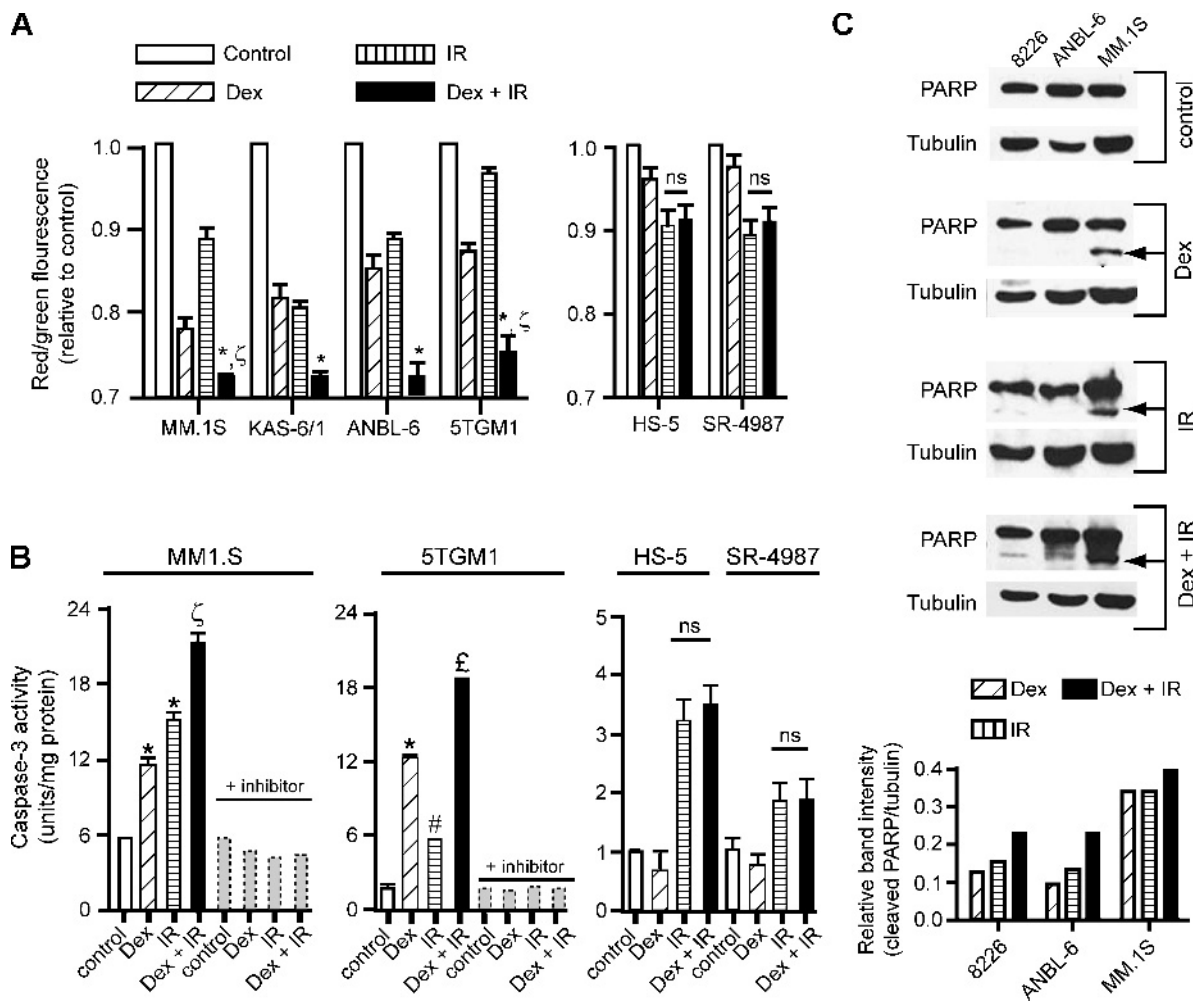

Figure 2. Dex and radiation induce cell death of myeloma cell lines by apoptotic pathway. (A) JC-1 fluorescence in myeloma and BMSCs with Dex (5 μM) and/or radiation (6 Gy) treatments at 6 hours after radiation. The data presented are the triplicate averages of the fluorescence ratio ± SD and are representative of two independent experiments. For specific cell lines, *$P < .01$ *versus* Dex, $^{\zeta}P < .005$ *versus* IR. ns indicates not significant. (B) Activity of caspase-3 in myeloma (MM.1S, 5TGM1) and BMSCs (HS-5, SR-4987) treated with Dex and/or radiation. The specificity of caspase-3 activation was confirmed with the N-Ac-Asp-Glu-Val-Asp-CHO caspase-3 inhibitor. Values presented are the mean of triplicate values ± SD and are representative of two independent experiments. *$P < .001$ *versus* control, $^{\zeta}P < .001$ *versus* Dex or IR, $^{\#}P < .05$ *versus* control, $^{\pounds}P < .001$ *versus* Dex or IR. ns indicates not significant. (C) Western blot analysis of PARP in myeloma cells (8226, ANBL-6, MM.1S) after Dex (5 μM) and/or radiation (6 Gy). For each treatment, top panels show full-length and cleaved PARP fragment (shown by arrows) and bottom panels show tubulin loading control. The blot shown is a representative of three independent blots. Values of densitometric analysis of cleaved PARP (normalized to tubulin) are shown.
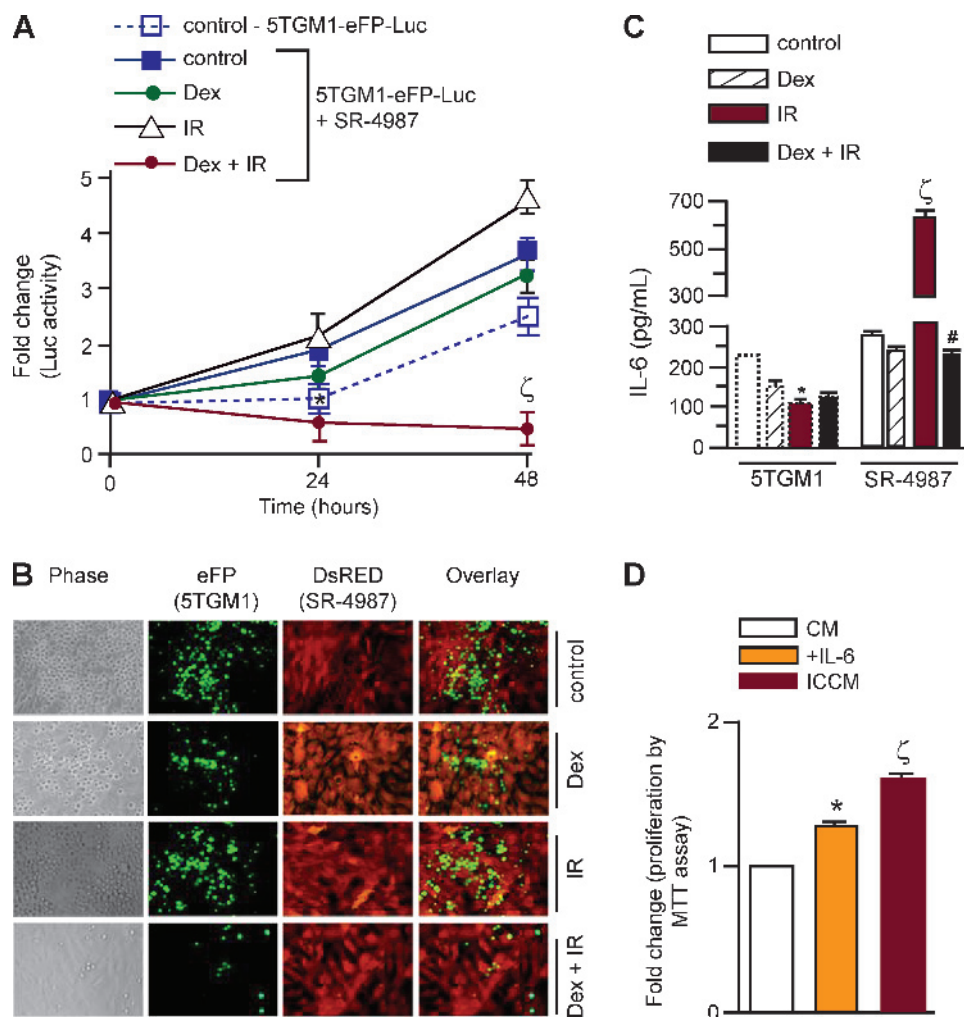
Figure 3. Dex potentiates radiation-mediated killing of myeloma cells cocultured with BMSCs and inhibits IL-6 release from irradiated BMSCs. (A) 5TGM1-eFP-Luc cells cultured alone or with SR-4987 BMSCs; cocultures were treated with Dex ($5\,\mu$M) and/or radiation (6 Gy), and luciferase (Luc) activity was measured at 24 or 48 hours after radiation. Values plotted are mean ± SD of triplicate samples and are representative of two independent experiments. Results are presented as fold change in Luc activity relative to time 0 (the latter set to 1). *$P < .05$ *versus* control or IR alone, $^{\zeta}P < .005$ *versus* control, Dex alone, or IR alone. (B) Fluorescence images of eFP (5TGM1) and DsRed (SR-4987) in cocultures at 24 hours after treatment with Dex and/or radiation. Images of untreated control are included. Each photograph is representative of three wells. Original magnification, ×40. (C) Quantification of IL-6 in culture supernatant by ELISA at 24 hours after 6-Gy radiation treatment of myeloma (5TGM1) or BMSCs (SR-4987), with or without Dex ($5\,\mu$M for 24 hours) pretreatment. Results are presented as IL-6 in picograms per milliliter (mean of triplicates ± SD). *$P < .05$ *versus* 5TGM1 control, $^{\zeta}P < .005$ *versus* SR-4987 control, $^{\#}P < .005$ *versus* IR. (D) Proliferation of 5TGM1 myeloma cells with exogenous IL-6 or SR-4987 conditioned medium from nonirradiated (CM) or irradiated cells (ICCM). MTT activity at 48 hours in untreated controls was set to 1, and results are shown as fold change over this activity. Results are representative of two independent experiments. *$P = .05$ *versus* control, $^{\zeta}P < .005$ *versus* control.

Table 1. BLI-Based Quantitation of Myeloma Burden in Live Mice as Indicative of Responses to Dex and/or 153-Sm-EDTMP Treatments.

Groups	Photons/sec/cm^2 ($\times 10^5$)	
	Day 18 (Mean ± SD)	Day 24 (Mean ± SD)
PBS	325.3 ± 22.2	1002.3 ± 134.2
Dex	206.3 ± 55.6	808.7 ± 60.3
153-Sm-EDTMP	203.0 ± 58.2	711.9 ± 109.4
Dex + 153-Sm-EDTMP	178.8 ± 29.1	320.9 ± 52.7

5TGM1-Luc cells were injected intravenously into mice on day 0. Treatment was started on day 12 after tumor inoculation and consisted of Dex and/or 153-Sm-EDTMP treatments as described in Materials and Methods. BLI signals from the entire abdominal area were calculated using the software Living Image (Xenogen). The data represent averaged luminescence intensity from six mice per group (±SD) and are displayed as photons per second after normalizing for the baseline luminescence intensity acquired from normal healthy mice.

prolonged median survival to 29 days ($P < .05$ *vs* control) and 31 days ($P < .005$ *vs* control), respectively. With a combination of Dex with 153-Sm-EDTMP, the median survival time increased to 44 days ($P = .001$ *vs* control and $P < .005$ *vs* 153-Sm-EDTMP or Dex alone; log rank test). Overall, the BLI and survival studies corroborate our *in vitro* results and show that Dex combined with radiotherapy results in significantly increased killing of BM-resident tumor cells.

To determine whether Dex was affecting 153-Sm-EDTMP–induced radiotoxicity to hematopoietic system *in vivo*, we analyzed complete blood cell counts. When Dex was combined with 153-Sm-EDTMP, the radiation-induced hematopoietic toxicity to both platelets (Figure 4B) and granulocytes (Figure 4C) was significantly less pronounced. For platelets, a nadir value of 190.7 ± 45.1 ($\times 10^9$/L) was seen on day 18 with 153-Sm-EDTMP alone that was significantly improved
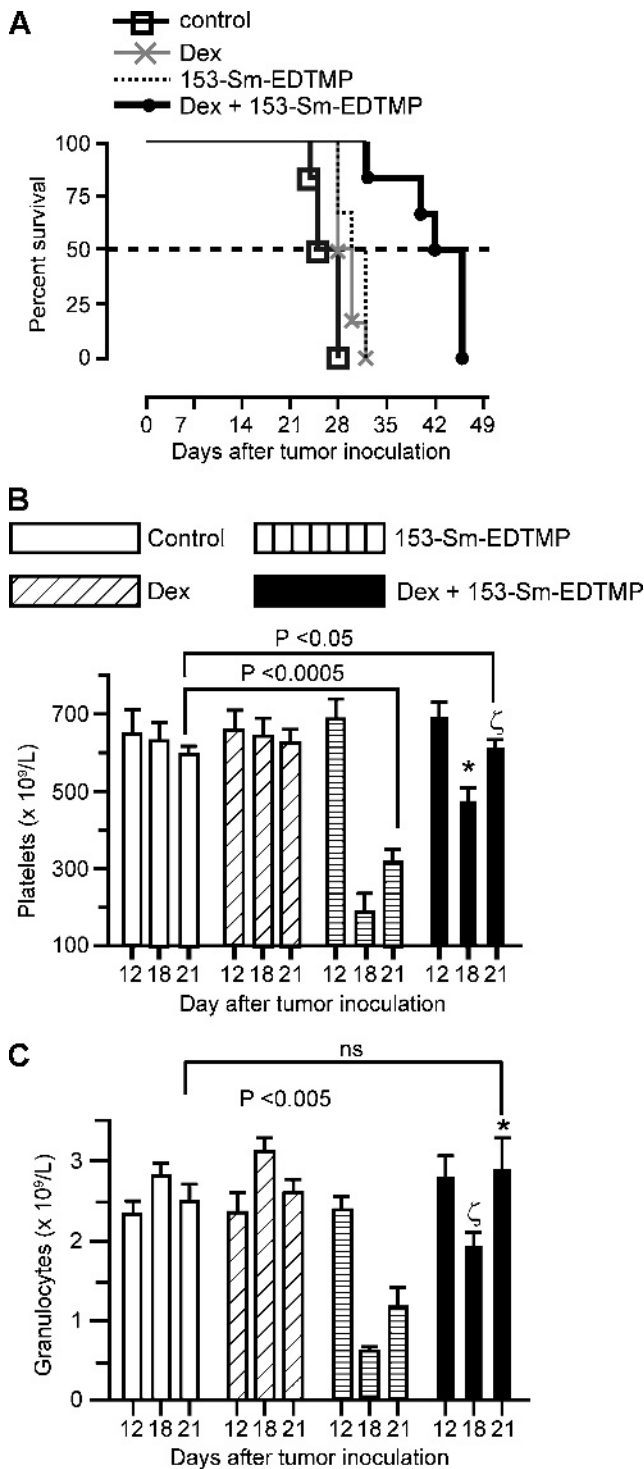
Figure 4. *In vivo* effect of Dex and/or 153-Sm-EDTMP on the survival and peripheral blood counts in 5TGM1-Luc model. (A) Kaplan-Meier survival curves for mice treated with one cycle of Dex and/or 153-Sm-EDTMP relative to survival in the untreated control group. Peripheral blood cell counts of platelet (B) and granulocyte (C) numbers on days 12, 18, and 21 after tumor implantation in various groups shown in panel A. Cell numbers are expressed as the mean ± SD. *P = .0001 *versus* 153-Sm-EDTMP, ζP < .0001 *versus* 153-Sm-EDTMP on respective days.

by combining Dex with 153-Sm-EDTMP (466.3 ± 42.1 [×10^9/L], P = .0001). A similar protection of platelet counts was seen on day 21 with values of 321.1 ± 29.1 and 601.2 ± 28.2 (× 10^9/L) for 153-Sm-EDTMP and Dex + 153-Sm-EDTMP, respectively (P < .0001). Dex was also found to be effective in rescuing peripheral granulocyte counts from radiotoxicity. In mice treated with 153-Sm-EDTMP alone, a severe granulocytosis was seen on day 18 that was significantly alleviated with Dex plus 153-Sm-EDTMP. Furthermore, on day 21, the granulocyte counts in mice receiving Dex + 153-Sm-EDTMP was comparable to those in the untreated control group, whereas the counts in mice receiving 153-Sm-EDTMP alone remained significantly repressed (P < .005).

From this *in vivo* study, we conclude that Dex increases 153-Sm-EDTMP–mediated killing of myeloma cells and ameliorates radiation toxicity to BM hematopoietic system. On the basis of the observation that Dex does not radiosensitize BMSCs (Figure 1*C*) that are known to provide a structural scaffold for BM hematopoiesis [48], Dex could be protecting specialized BM niches thereby restoring hematopoiesis. Also, combining Dex with radiotherapy may be protecting normal hematopoietic stem and progenitor cell population from bystander radiation toxicity culminating in less severe myelosuppression.

Combining Dex with 153-Sm-EDTMP Enables Administration of Two Cycles of 153-Sm-EDTMP with Further Prolongation of the Survival of 5TGM1 Bearing Mice

We next compared the efficacy of one, *versus* two-cycle therapy with Dex and/or 153-Sm-EDTMP (Figure 5). The control animals
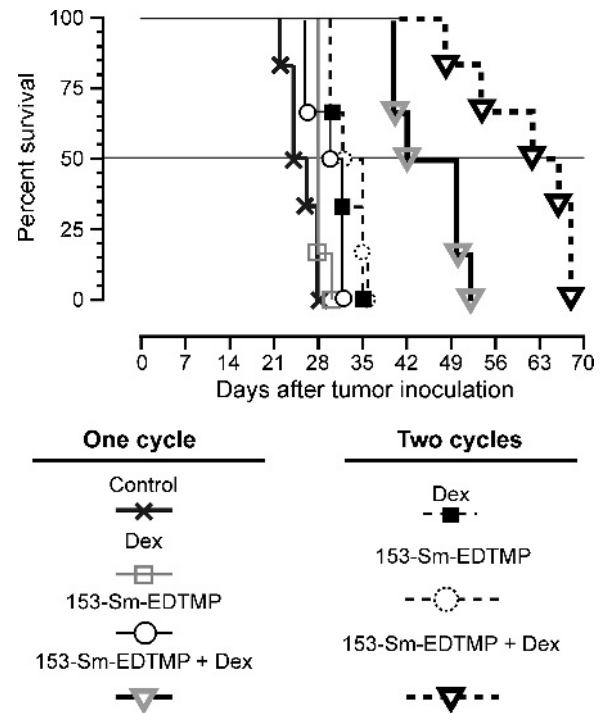

Figure 5. Kaplan-Meier survival curves for 5TGM1-Luc mice subjected to either one or two cycles of the Dex and/or 153-Sm-EDTMP treatments. The first cycle of treatment was initiated on day 12 after tumor injection. In the two-cycle regimen, the second cycle of treatment was initiated on day 22 where Dex was given on days 22 to 26 and 153-Sm-EDTMP was given on day 23. Mice were followed until they reached the humane end point.

exhibited a median survival of 25 to 26.5 days. One- and two-cycle regimens with Dex showed a prolongation of the median survival to 28 days (P = .005 vs control) and 32 days (P < .005 vs one-cycle regimen). Treatment with one cycle of 153-Sm-EDTMP resulted in a modest increase in the median survival time (to 31 days) compared with that of the control (25 days, P < .005). Two cycles of 153-Sm-EDTMP did not provide any further increase of the median survival (33.5 days, P = ns between one- and two-cycle protocols) and mice showed significant loss in body weight and other signs of radiotoxicity (data not shown). With Dex and 153-Sm-EDTMP, the median survival of 46 days was seen with the one-cycle regimen (P = .0001, relative to untreated controls) that was increased to 64 days with two cycles of Dex plus 153-Sm-EDTMP (P < .01 relative to one cycle of Dex plus 153-Sm-EDTMP). This $in\ vivo$ study indicates that Dex may be effectively combined with 153-Sm-EDTMP for repeat dosing of radionuclide to augment the overall therapeutic efficacy of skeletal targeted radiotherapy in the treatment of systemic MM.

Dex Induces Myeloma Cell Killing by Increasing Steady-State Levels Pro-oxidants

As myeloma cells may have higher steady-state levels of pro-oxidants [31], we next analyzed if treatment with Dex and radiotherapy would result in a further increase in oxidative stress in myeloma cells rendering them more susceptible to undergo radiation-induced cell killing. Clonogenic survival was performed in myeloma cells that were either treated with Dex or cotreated with NAC (a clinically relevant thiol antioxidant) or the combination of polyethylene glycol (PEG)–conjugated SOD (scavenges $O_2^{\bullet-}$) and PEG-catalase (scavenges H_2O_2) [49]. Treatment with Dex resulted in approximately a 60% and a 50% inhibition in the clonogenic ability of ANBL-6 and 5TGM1 cells, respectively (Figure 6A). Both NAC pretreatment and combination of PEG-SOD and PEG-CAT significantly rescued Dex-mediated clonogenic cell killing of both cell lines. Overall, Figure 6A demonstrates that induction of oxidative stress, mediated by ROS, is an important component in Dex-mediated killing of myeloma cells.

Combination of Dex with Radiation Treatment Results in Increased Oxidative Stress in Myeloma Cells and Not BMSCs

To determine whether ROS production is involved in Dex-mediated increased killing of myeloma cells by radiation, DHE oxidation was measured as a surrogate for $O_2^{\bullet-}$ (Figure 6B). Compared with untreated cells, the $O_2^{\bullet-}$ production (determined by PEG-SOD inhibitable DHE oxidation) was significantly elevated in both Dex- or radiation-treated 5TGM1 cells (P < .01). This $O_2^{\bullet-}$ production was significantly increased with combination treatment of Dex plus radiation (P < .01). In BMSCs, Dex marginally increased the $O_2^{\bullet-}$ production, yet radiation was found to increase DHE fluorescence significantly (P < .001). However, combined treatment of Dex and radiation did not further increase the $O_2^{\bullet-}$ production in BMSCs.

We next assessed the impact of Dex and/or radiation treatment on the steady-state levels of intracellular pro-oxidants by $H_2DCF-DA$ oxidation. PEG-CAT was used to confirm the specificity of the signal for H_2O_2 (Figure 6C). In 5TGM1 cells, relative to the untreated control, treatment with Dex or radiation resulted in increased PEG-CAT-inhibitable $H_2DCF-DA$ oxidation that was further enhanced in response to the Dex plus radiation treatment (P < .0001 vs radiation or Dex), indicating that Dex is augmenting radiation-induced increases in H_2O_2 generation in myeloma cells. Furthermore, Dex did not increase radiation-induced H_2O_2 production in BMSCs (Figure 6C).

Overall, the results of Figure 6 show that myeloma cells are subject to increased oxidative stress by Dex treatment that is further increased with the combined treatment of Dex plus radiation.

Dex Mitigates Radiation-Induced Changes in Pro-oxidant Levels and Protects the Normal Hematopoietic Stem and Progenitor Cells from Radiotoxicity

BM harbors the hematopoietic system, and any radiation-based therapeutic strategy directed toward myeloma cells is expected to cause acute myelosuppression by irradiating and depleting the hematopoietic stem and precursor cell pools [50]. On the basis of Dex-mediated protection of peripheral blood cell counts (Figure 4, B and C), we next determined whether Dex could protect the BM hematopoietic system from radiotoxicity by reducing radiation-induced pro-oxidant production.

Primary HSCs and HPCs were isolated from C57BL/6 mice, and a representative sorting pattern is shown in Figure 7A. These normal cells were treated $ex\ vivo$ with Dex and/or radiation and analyzed for steady-state levels of pro-oxidants (Figure 7B). Compared with the untreated control, treatment with Dex or radiation increased the steady-state levels of ROS in HSCs that was attenuated by NAC pretreatment. When HSCs were treated with Dex plus radiation, a decreased steady-state level of pro-oxidants was noted relative to the level in radiation alone (P < .05), suggesting that Dex can inhibit the pro-oxidant generation induced by radiation. Although the combination treatment of Dex plus radiation did not bring the pro-oxidant levels in HSCs down to the baseline level, no significant difference was noted when the oxidation of $H_2DCF-DA$ was compared between Dex or Dex plus radiation treatments. Studies were also performed in the primary HPCs where Dex and radiation alone increased ROS, relative to control. On combination treatment with Dex plus radiation, the pro-oxidant levels were significantly lower than those seen with radiation alone (P < .0005). The results in Figure 7B suggest that HSCs and HPCs are highly susceptible to radiation-induced up-regulation of steady-state levels of pro-oxidants and that Dex can significantly inhibit radiation-induced oxidative stress in these hematopoietic stem/progenitor cells.

We next determined whether the Dex-mediated inhibition of steady-state levels of pro-oxidants might lead to a clonogenic survival benefit after radiation therapy (Figure 7C). Compared with untreated cells, radiation inhibited the colony-forming ability of both HSCs and HPCs (P < .0001 for each cell type). HSCs were found to be relatively more resistant to radiation toxicity than HPCs presumably because of the quiescent nature of this cell type. Compared with radiation treatment alone, when HSCs or HPCs were treated with Dex plus radiation, the clonogenic survival of both cell types was increased (P < .01). This result corroborates the findings shown in Figure 7B and suggests that the proposed combination of Dex plus radiation can inhibit radiation-induced oxidative stress and improve clonogenic survival of HSCs and HPCs.

Discussion

Dex is among one of the most clinically effective drugs in myeloma therapy. In lymphoid malignancies, Dex-induced apoptotic cell death pathways have been partially deciphered [20,21]. Our results show that Dex treatment results in the activation of the mitochondrial apoptotic cascade in myeloma cells (Figure 2), further substantiating the role of mitochondrial dysfunction in Dex-mediated apoptosis. Studies have linked Dex-induced apoptosis and oxidative stress using a thymic lymphoma cell line where clones resistant to H_2O_2 (by catalase overexpression or selection of H_2O_2-resistant clones) showed Dex
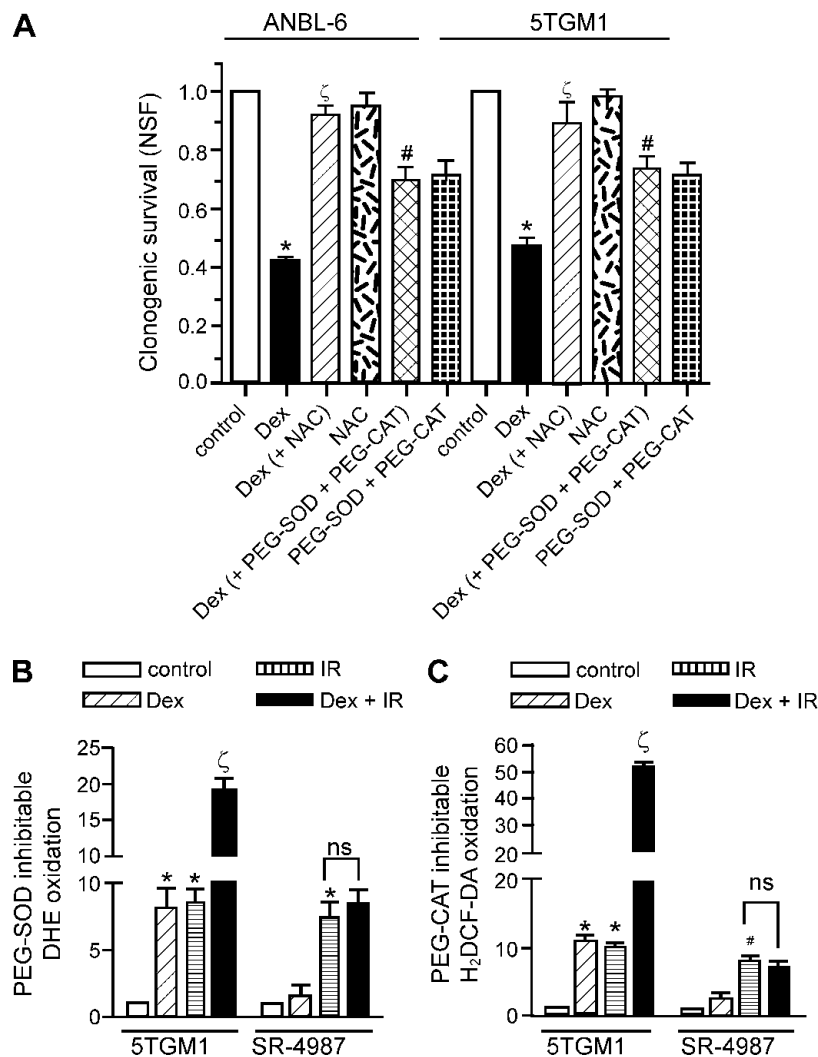
Figure 6. Dex induces ROS-mediated clonogenic cell death of myeloma cells and potentiates radiation-induced ROS levels in myeloma cells but not in BMSCs. (A) Clonogenic survival of myeloma (ANBL-6 or 5TGM1) after Dex (5 μM for 24 hours) combined with or without NAC or PEG-SOD and PEG-CAT. Results are expressed as the NSF of triplicate cloning wells and are representative of two independent experiments. *$P <$ .001 *versus* Dex, $^{\zeta}P <$ .001 *versus* NAC, $^{\#}P <$ .01 *versus* Dex. Effect of Dex (5 μM) and/or 6-Gy radiation in myeloma (5TGM1) and BMSCs (SR-4987) on the steady-state levels of (B) $O_2^{\bullet-}$ in the presence of PEG-SOD (*$P <$ .01 *vs* control, $^{\zeta}P <$ .01 *vs* Dex or radiation) or (C) H_2O_2 in the presence of PEG-CAT (*$P <$ .005 *vs* control, $^{\zeta}P <$ .0001 *vs* Dex or radiation). For panels B and C, values are averages of triplicate $\pm$ SD and calculated by subtracting the fluorescence value measured in the presence and absence of PEG-SOD or PEG-CAT, respectively. ns indicates not significant.

cross-resistance [51]. Dex treatment has been shown to upregulate the messenger RNA expression of glutathione *S*-transferase and downregulate the messenger RNA of thioredoxin, glutathione peroxidase, catalase, and superoxide dismutase in T lymphocytes [33,34]. However, in MM, a causal role for oxidative stress in Dex-induced tumor cell death has not been firmly established. Chauhan et al. [36] showed that Dex-induced apoptosis of myeloma cells is independent of $O_2^{\bullet-}$ production. However, it was recently shown that newly diagnosed myeloma patients treated with Dex exhibit gene expression changes indicative of oxidative stress [37]. In the current report, we show for the first time that besides various other known myeloma cell death mechanism(s), Dex increases oxidative stress–induced clonogenic cell killing in myeloma cells (Figure 6A).

Newly diagnosed MM patients have higher circulating levels of malondialdehyde indicative of lipid peroxidation and lower levels of antioxidant enzymes (superoxide dismutases, glutathione peroxidases,

and catalase) in erythrocytes [30–32]. Because myeloma patients may be under systemic oxidative stress at diagnosis, treatment with agents that selectively induce oxidative stress (chemotherapy and radiotherapy) in tumor cells may significantly enhance their oxidative cytolysis. In support of this hypothesis, our *in vitro* studies with combined exposure to Dex and radiation clearly show an increase in Dex-induced oxidative stress (Figure 6, *B* and *C*) that seems to be causally related to a significant decrease in clonogenic survival of myeloma cells (Figure 1*C*). Furthermore, Dex-induced increases in oxidative stress and cell killing were not noted in BMSCs, thus not worsening hematopoietic recovery after radiotherapy as also seen by peripheral blood cell counts (Figure 4, *B* and *C*). This leads to the speculation that the combination of Dex with radiation may increase the therapeutic index of skeletal targeted radiotherapy in MM by selectively inducing oxidative stress in cancer cells.

Our studies show that in contrast to myeloma cells, Dex inhibited radiation-induced oxidative stress in normal hematopoietic stem and

progenitor cells (Figure 7*B*). We hypothesize that Dex attenuates radiation-induced cytotoxicity to HSCs and HPCs by decreasing steady-state levels of pro-oxidants to a threshold level that may be aiding in improved hematopoietic reconstitution. Our *in vivo* studies show that Dex cotreatment results in less severe and faster peripheral

Figure 7. Dex inhibits radiation-induced oxidative stress and alleviates radiation toxicity in HSCs and HPCs. (A) Representative flow cytometry profile of isolation of HPCs and HSCs used in panels B and C. (B) Intracellular levels of pro-oxidants in HSCs or HPCs treated with Dex and/or radiation with or without NAC as measured by H_2DCF-DA oxidation. The values are normalized to those for untreated controls and are representative of two independent experiments. $*P < .001$ *versus* control, $^\zeta P < .05$ *versus* radiation, $^\tau P < .0005$ *versus* radiation. (C) Clonogenic survival of HSCs and HPCs treated with Dex and/or radiation normalized to the survival of untreated control cell populations. Three cloning replicates were counted for each treatment and results are representative of two independent experiments. $*P < .0001$ *versus* control, $^\zeta P < .01$ *versus* radiation.

blood reconstitution of blood cell types (granulocytes and platelets) compared with radiotherapy alone (Figure 4, *B* and *C*). In erythroid cells, a hematoprotective role of Dex with chemotherapeutic drugs has been shown where it stimulates a sustained proliferation of immature cells and delays their differentiation [52]. Recently, ROS has been shown to act as a positive regulator of hematopoietic reconstitution by upregulating vascular cell adhesion molecule 1 expression on endothelial cells [53]. To assess whether Dex was protecting hematopoietic stem/progenitor cells from radiation-induced damage, clonogenic survival of HSC/HPC was performed where the progenitor number of different lineages (myeloid and lymphoid lineages, common myeloid progenitor, and common lymphoid progenitor subsets) was collectively analyzed. Compared with radiation alone, Dex cotreatment showed higher clonogenic survival of both HSCs and HPCs (Figure 7*C*), suggesting that the improved *in vivo* restoration of normal hematopoiesis after combination treatment with Dex plus 153-Sm-EDTMP could be partially rendered by Dex-mediated radioprotection of HSCs and HPCs.

In the present study, we have focused on the myeloma cell proproliferative cytokine IL-6 [54] that is released by irradiated BMSCs (Figure 3*C*). It is well established that radiation treatment upregulates redox-sensitive transcriptional factors (i.e., NF-κB and AP-1) [55] that have been shown to increase IL-6 production in MM cells [27]. Dex has also been shown to inhibit radiation-induced IL-6 up-regulation in fibroblasts [56]. Mechanistically, Dex can inhibit constitutive and radiation-induced IL-6 production by binding and inhibiting NF-κB [57] or upregulating the transcription of IκB [58] or glucocorticoid-induced leucine zipper that can inhibit NF-κB and AP-1 [59–61]. Using myeloma-BMSCs coculture studies, we show that IL-6 as well as other radiation-induced pro-inflammatory cytokines may be stimulating myeloma growth and proliferation, and this paracrine cytokine stimulation can be effectively inhibited by Dex (Figure 3*C*) with selective radiosensitization of myeloma cells.

To evaluate the efficacy of the proposed combination therapy for Dex plus radiation, studies were extended in an animal model (Figures 4 and 5). We have previously shown that the *in vitro* cell killing of a chemoradiotherapy regimen with γ-radiation can be effectively reproduced *in vivo* with 153-Sm-EDTMP [42]. Cotreatment of Dex with 153-Sm-EDTMP resulted in inhibition of myeloma disease progression and improved survival (Figure 4). With 153-Sm-EDTMP, 87.5% of the radiation dose would be delivered to the BM in three half-lives (>6 days). We therefore tested a two-cycle protocol where 153-Sm-EDTMP was administered 10 days apart that also gave time for Dex-mediated recovery of the peripheral blood counts. A two-cycle protocol of Dex plus 153-Sm-EDTMP prolonged the survival over one-cycle protocol (Figure 5), indicating that cotreatment with Dex may be used for designing a repeat dosing regimen of bone-seeking radionuclide and/or for escalation of radiation dose to improve the therapeutic outcome of MM.

Dex is among one of the most clinically effective drugs in myeloma therapy [62] that is used in chemotherapy protocols with novel molecularly targeted agents such as bortezomib and thalidomide [63]. When combined with radiation treatment, an increased myeloma cell killing of thalidomide [13] and bortezomib [14,15] has been noted. In our previous study, the combination of bortezomib with 153-Sm-EDTMP resulted in the prolongation of survival without increasing the myelosuppressive effects of 153-Sm-EDTMP [42]. The current report shows that the combination of 153-Sm-EDTMP with Dex selectively radiosensitizes myeloma cells *in vivo* and partially alleviates radiotoxicity
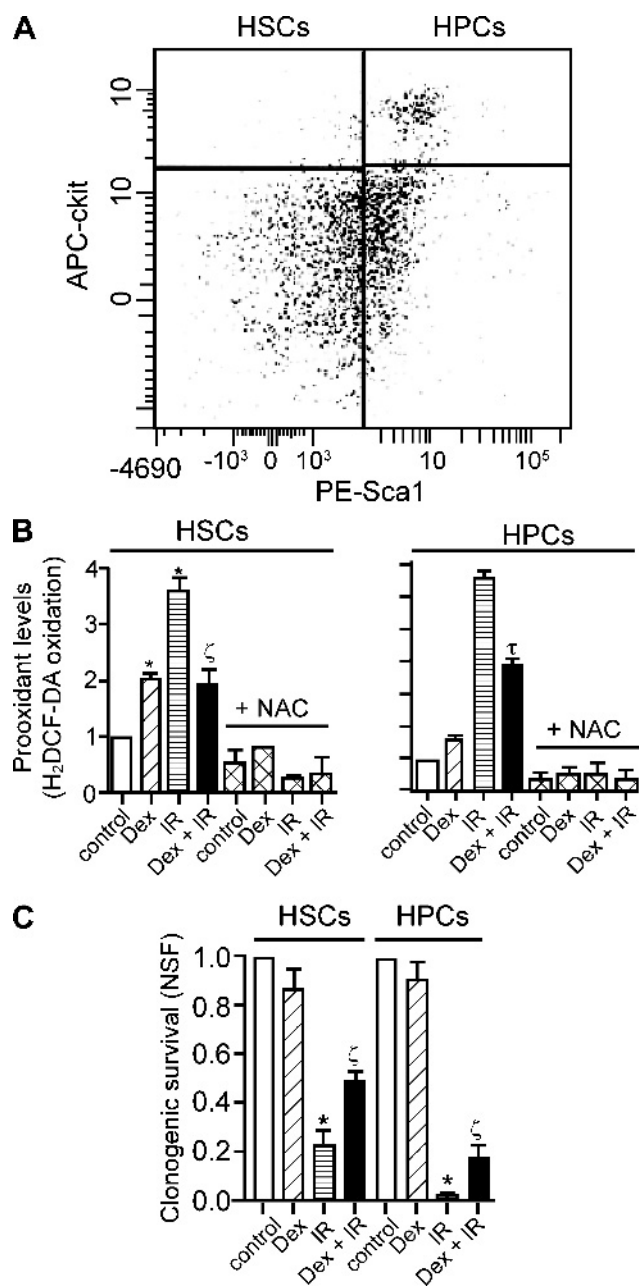
toward the BM hematopoietic system. Mechanistically, we show that the combination of radiotherapy and Dex selectively enhances killing of myeloma cells while protecting normal BM hematopoiesis through a mechanism that involves selective increases in oxidative stress in myeloma cells. The results of this study can be extended for myeloma therapy in combination with bortezomib, thalidomide, or other novel biologic agents that may enhance the potency of Dex and/or radiation in killing myeloma cells. To our knowledge, this is the first report showing that Dex significantly and specifically enhances radiation-induced oxidative stress and killing of myeloma cells in monocultures, direct cocultures, and *in vivo* in a myeloma model. Our findings in normal tissues suggest that Dex decreases hematotoxicity and increases the overall therapeutic index of radiotherapy in MM. This study provides a potential new avenue for therapeutic use of Dex in designing protocols for myeloma therapy. Furthermore, the proposed combination of Dex and radiation can be tested in other malignancies because both these treatment modalities are widely used in various cancers.

Acknowledgments

References

[1] Mill WB (1975). Radiation therapy in multiple myeloma. *Radiology* **115**, 175–178.

[2] Bosch A and Frias Z (1988). Radiotherapy in the treatment of multiple myeloma. *Int J Radiat Oncol Biol Phys* **15**, 1363–1369.

[3] Kilciksiz S, Celik OK, Pak Y, Demiral AN, Pehlivan M, Orhan O, Tokatli F, Agaoglu F, Zincircioglu B, Atasoy BM, et al. (2008). Clinical and prognostic features of plasmacytomas: a multicenter study of Turkish Oncology Group–Sarcoma Working Party. *Am J Hematol* **83**, 702–707.

[4] Lewanski CR, Bates T, Bowen J, and Ashford RF (1999). Solitary bone plasmacytoma: management of isolated local relapse following radiotherapy. *Clin Oncol (R Coll Radiol)* **11**, 348–351.

[5] Goel A, Dispenzieri A, Witzig TE, and Russell SJ (2006). Enhancing the therapeutic index of radiation in multiple myeloma. *Drug Discov Today Dis Mech* **3**, 515–522.

[6] Chatterjee M, Chakraborty T, and Tassone P (2006). Multiple myeloma: monoclonal antibodies–based immunotherapeutic strategies and targeted radiotherapy. *Eur J Cancer* **42**, 1640–1652.

[7] Wong JY, Liu A, Schultheiss T, Popplewell L, Stein A, Rosenthal J, Essensten M, Forman S, and Somlo G (2006). Targeted total marrow irradiation using three-dimensional image-guided tomographic intensity–modulated radiation therapy: an alternative to standard total body irradiation. *Biol Blood Marrow Transplant* **12**, 306–315.

[8] Wong JY, Rosenthal J, Liu A, Schultheiss T, Forman S, and Somlo G (2009). Image-guided total-marrow irradiation using helical tomotherapy in patients with multiple myeloma and acute leukemia undergoing hematopoietic cell transplantation. *Int J Radiat Oncol Biol Phys* **73**, 273–279.

[9] Anderson PM, Wiseman GA, Dispenzieri A, Arndt CA, Hartmann LC, Smithson WA, Mullan BP, and Bruland OS (2002). High-dose samarium-153 ethylene diamine tetramethylene phosphonate: low toxicity of skeletal irradiation in patients with osteosarcoma and bone metastases. *J Clin Oncol* **20**, 189–196.

[10] Dispenzieri A, Wiseman GA, Lacy MQ, Geyer S, Litzow MR, Tefferi A, Inwards DJ, Micallef IN, Ansell S, Gastineau DA, et al. (2003). A phase II study of high dose 153-samarium EDTMP (153-sm EDMTP) and melphalan for peripheral stem cell transplantation (PBSCT) in multiple myeloma (MM). *Blood* **102**, 982a-a.

[11] Dispenzieri A, Wiseman GA, Lacy MQ, Hayman SR, Kumar SK, Buadi F, Dingli D, Laumann KM, Allred J, Geyer SM, et al. (2010). A phase II study of (153)Sm-EDTMP and high-dose melphalan as a peripheral blood stem cell conditioning regimen in patients with multiple myeloma. *Am J Hematol* **85**, 409–413.

[12] Abruzzese E, Iuliano F, Trawinska MM, and Di Maio M (2008). ^{153}Sm: its use in multiple myeloma and report of a clinical experience. *Expert Opin Investig Drugs* **17**, 1379–1387.

[13] Marchand V, Decaudin D, Servois V, and Kirova YM (2008). Concurrent radiation therapy and lenalidomide in myeloma patient. *Radiother Oncol* **87**, 152–153.

[14] Berenson JR, Yellin O, Patel R, Duvivier H, Nassir Y, Mapes R, Abaya CD, and Swift RA (2009). A phase I study of samarium lexidronam/bortezomib combination therapy for the treatment of relapsed or refractory multiple myeloma. *Clin Cancer Res* **15**, 1069–1075.

[15] Berges O, Decaudin D, Servois V, and Kirova YM (2008). Concurrent radiation therapy and bortezomib in myeloma patient. *Radiother Oncol* **86**, 290–292.

[16] Palumbo A and Gay F (2009). How to treat elderly patients with multiple myeloma: combination of therapy or sequencing. *Hematology Am Soc Hematol Educ Program*, 566–577.

[17] Turesson I, Velez R, Kristinsson SY, and Landgren O (2010). Patterns of multiple myeloma during the past 5 decades: stable incidence rates for all age groups in the population but rapidly changing age distribution in the clinic. *Mayo Clin Proc* **85**, 225–230.

[18] Alexanian R, Dimopoulos MA, Delasalle K, and Barlogie B (1992). Primary dexamethasone treatment of multiple myeloma. *Blood* **80**, 887–890.

[19] Rajkumar SV, Gertz MA, Kyle RA, and Greipp PR (2002). Current therapy for multiple myeloma. *Mayo Clin Proc* **77**, 813–822.

[20] Frankfurt O and Rosen ST (2004). Mechanisms of glucocorticoid-induced apoptosis in hematologic malignancies: updates. *Curr Opin Oncol* **16**, 553–563.

[21] Greenstein S, Ghias K, Krett NL, and Rosen ST (2002). Mechanisms of glucocorticoid-mediated apoptosis in hematological malignancies. *Clin Cancer Res* **8**, 1681–1694.

[22] Chauhan D, Pandey P, Hideshima T, Treon S, Raje N, Davies FE, Shima Y, Tai YT, Rosen S, Avraham S, et al. (2000). SHP2 mediates the protective effect of interleukin-6 against dexamethasone-induced apoptosis in multiple myeloma cells. *J Biol Chem* **275**, 27845–27850.

[23] Richardson PG, Sonneveld P, Schuster MW, Irwin D, Stadtmauer EA, Facon T, Harousseau JL, Ben-Yehuda D, Lonial S, Goldschmidt H, et al. (2005). Bortezomib or high-dose dexamethasone for relapsed multiple myeloma. *N Engl J Med* **352**, 2487–2498.

[24] Zangari M, Tricot G, Polavaram L, Zhan F, Finlayson A, Knight R, Fu T, Weber D, Dimopoulos MA, Niesvizky R, et al. (2010). Survival effect of venous thromboembolism in patients with multiple myeloma treated with lenalidomide and high-dose dexamethasone. *J Clin Oncol* **28**, 132–135.

[25] Spitz DR, Azzam EI, Li JJ, and Gius D (2004). Metabolic oxidation/reduction reactions and cellular responses to ionizing radiation: a unifying concept in stress response biology. *Cancer Metastasis Rev* **23**, 311–322.

[26] Grigorieva I, Thomas X, and Epstein J (1998). The bone marrow stromal environment is a major factor in myeloma cell resistance to dexamethasone. *Exp Hematol* **26**, 597–603.

[27] Xiao W, Hodge DR, Wang L, Yang X, Zhang X, and Farrar WL (2004). NF-κB activates IL-6 expression through cooperation with c-Jun and IL6-AP1 site, but is independent of its IL6-NFκB regulatory site in autocrine human multiple myeloma cells. *Cancer Biol Ther* **3**, 1007–1017.

[28] Kawano M, Hirano T, Matsuda T, Taga T, Horii Y, Iwato K, Asaoku H, Tang B, Tanabe O, Tanaka H, et al. (1988). Autocrine generation and requirement of BSF-2/IL-6 for human multiple myelomas. *Nature* **332**, 83–85.

[29] Hodge DR, Xiao W, Peng B, Cherry JC, Munroe DJ, and Farrar WL (2005). Enforced expression of superoxide dismutase 2/manganese superoxide dismutase disrupts autocrine interleukin-6 stimulation in human multiple myeloma cells and enhances dexamethasone-induced apoptosis. *Cancer Res* **65**, 6255–6263.

[30] Kuku I, Aydogdu I, Bayraktar N, Kaya E, Akyol O, and Erkurt MA (2005). Oxidant/antioxidant parameters and their relationship with medical treatment in multiple myeloma. *Cell Biochem Funct* **23**, 47–50.

[31] Sharma A, Tripathi M, Satyam A, and Kumar L (2009). Study of antioxidant levels in patients with multiple myeloma. *Leuk Lymphoma* **50**, 809–815.

[32] Zima T, Spicka I, Stipek S, Crkovska J, Platenik J, Merta M, Nemecek K, and Tesar V (1996). Lipid peroxidation and activity of antioxidative enzymes in patients with multiple myeloma. *Cas Lek Cesk* **135**, 14–17.

[33] Baker AF, Briehl MM, Dorr R, and Powis G (1996). Decreased antioxidant defence and increased oxidant stress during dexamethasone-induced apoptosis: bcl-2 prevents the loss of antioxidant enzyme activity. *Cell Death Differ* **3**, 207–213.

[34] Briehl MM, Cotgreave IA, and Powis G (1995). Downregulation of the antioxidant defence during glucocorticoid-mediated apoptosis. *Cell Death Differ* **2**, 41–46.

[35] Jaramillo MC, Frye JB, Crapo JD, Briehl MM, and Tome ME (2009). Increased manganese superoxide dismutase expression or treatment with manganese porphyrin potentiates dexamethasone-induced apoptosis in lymphoma cells. *Cancer Res* **69**, 5450–5457.

[36] Chauhan D, Li G, Sattler M, Podar K, Mitsiades C, Mitsiades N, Munshi N, Hideshima T, and Anderson KC (2003). Superoxide-dependent and -independent mitochondrial signaling during apoptosis in multiple myeloma cells. *Oncogene* **22**, 6296–6300.

[37] Burington B, Barlogie B, Zhan F, Crowley J, and Shaughnessy JD Jr (2008). Tumor cell gene expression changes following short-term *in vivo* exposure to single agent chemotherapeutics are related to survival in multiple myeloma. *Clin Cancer Res* **14**, 4821–4829.

[38] Dandona P, Mohanty P, Hamouda W, Aljada A, Kumbkarni Y, and Garg R (1999). Effect of dexamethasone on reactive oxygen species generation by leukocytes and plasma interleukin-10 concentrations: a pharmacodynamic study. *Clin Pharmacol Ther* **66**, 58–65.

[39] Ferrigno A, Gregotti C, Richelmi P, and Vairetti M (2010). Dexamethasone protects cultured rat hepatocytes against cadmium toxicity: involvement of cellular thiols. *In Vitro Cell Dev Biol Anim* **46**, 445–449.

[40] Baumeister P, Korn G, Berghaus A, Matthias C, and Harreus U (2009). Chemopreventive action of dexamethasone and alpha-tocopherol in oxidative stressed cells. *Cancer Detect Prev* **32**, 452–457.

[41] Wang Y, Liu L, Pazhanisamy SK, Li H, Meng A, and Zhou D (2010). Total body irradiation causes residual bone marrow injury by induction of persistent oxidative stress in murine hematopoietic stem cells. *Free Radic Biol Med* **48**, 348–356.

[42] Goel A, Dispenzieri A, Geyer SM, Greiner S, Peng KW, and Russell SJ (2006). Synergistic activity of the proteasome inhibitor PS-341 with non-myeloablative 153-Sm-EDTMP skeletally targeted radiotherapy in an orthotopic model of multiple myeloma. *Blood* **107**, 4063–4070.

[43] Goel A, Dispenzieri A, Greipp PR, Witzig TE, Mesa RA, and Russell SJ (2005). PS-341–mediated selective targeting of multiple myeloma cells by synergistic increase in ionizing radiation-induced apoptosis. *Exp Hematol* **33**, 784–795.

[44] Goel A, Carlson SK, Classic KL, Greiner S, Naik S, Power AT, Bell JC, and Russell SJ (2007). Radioiodide imaging and radiovirotherapy of multiple myeloma using VSV(Delta51)-NIS, an attenuated vesicular stomatitis virus encoding the sodium iodide symporter gene. *Blood* **110**, 2342–2350.

[45] Schmidmaier R, Baumann P, Emmerich B, and Meinhardt G (2006). Evaluation of chemosensitivity of human bone marrow stromal cells—differences between common chemotherapeutic drugs. *Anticancer Res* **26**, 347–350.

[46] Pessina A, Neri MG, Mineo E, Piccirillo M, Gribaldo L, Brambilla P, Zaleskis G, and Ujhazy P (1997). Expression of B cell markers on SR-4987 cells derived from murine bone marrow stroma. *Exp Hematol* **25**, 536–541.

[47] Hideshima T and Anderson KC (2002). Molecular mechanisms of novel therapeutic approaches for multiple myeloma. *Nat Rev Cancer* **2**, 927–937.

[48] Zhang J, Niu C, Ye L, Huang H, He X, Tong WG, Ross J, Haug J, Johnson T, Feng JQ, et al. (2003). Identification of the haematopoietic stem cell niche and control of the niche size. *Nature* **425**, 836–841.

[49] Zhu Y, Kalen AL, Li L, Lehmler HJ, Robertson LW, Goswami PC, Spitz DR, and Aykin-Burns N (2009). Polychlorinated-biphenyl–induced oxidative stress and cytotoxicity can be mitigated by antioxidants after exposure. *Free Radic Biol Med* **47**, 1762–1771.

[50] Mauch P, Constine L, Greenberger J, Knospe W, Sullivan J, Liesveld JL, and Deeg HJ (1995). Hematopoietic stem cell compartment: acute and late effects of radiation therapy and chemotherapy. *Int J Radiat Oncol Biol Phys* **31**, 1319–1339.

[51] Tome ME, Baker AF, Powis G, Payne CM, and Briehl MM (2001). Catalase-overexpressing thymocytes are resistant to glucocorticoid-induced apoptosis and exhibit increased net tumor growth. *Cancer Res* **61**, 2766–2773.

[52] von Lindern M, Zauner W, Mellitzer G, Steinlein P, Fritsch G, Huber K, Lowenberg B, and Beug H (1999). The glucocorticoid receptor cooperates with the erythropoietin receptor and c-Kit to enhance and sustain proliferation of erythroid progenitors *in vitro*. *Blood* **94**, 550–559.

[53] Lewandowski D, Barroca V, Duconge F, Bayer J, Van Nhieu JT, Pestourie C, Fouchet P, Tavitian B, and Romeo PH (2010). *In vivo* cellular imaging pinpoints the role of reactive oxygen species in the early steps of adult hematopoietic reconstitution. *Blood* **115**, 443–452.

[54] Podar K, Richardson PG, Hideshima T, Chauhan D, and Anderson KC (2007). The malignant clone and the bone-marrow environment. *Best Pract Res Clin Haematol* **20**, 597–612.

[55] Criswell T, Leskov K, Miyamoto S, Luo G, and Boothman DA (2003). Transcription factors activated in mammalian cells after clinically relevant doses of ionizing radiation. *Oncogene* **22**, 5813–5827.

[56] Beetz A, Messer G, Oppel T, van Beuningen D, Peter RU, and Kind P (1997). Induction of interleukin 6 by ionizing radiation in a human epithelial cell line: control by corticosteroids. *Int J Radiat Biol* **72**, 33–43.

[57] De Bosscher K, Schmitz ML, Vanden Berghe W, Plaisance S, Fiers W, and Haegeman G (1997). Glucocorticoid-mediated repression of nuclear factor-κB–dependent transcription involves direct interference with transactivation. *Proc Natl Acad Sci USA* **94**, 13504–13509.

[58] Ramdas J and Harmon JM (1998). Glucocorticoid-induced apoptosis and regulation of NF-κB activity in human leukemic T cells. *Endocrinology* **139**, 3813–3821.

[59] Eddleston J, Herschbach J, Wagelie-Steffen AL, Christiansen SC, and Zuraw BL (2007). The anti-inflammatory effect of glucocorticoids is mediated by glucocorticoid-induced leucine zipper in epithelial cells. *J Allergy Clin Immunol* **119**, 115–122.

[60] Grugan KD, Ma C, Singhal S, Krett NL, and Rosen ST (2008). Dual regulation of glucocorticoid-induced leucine zipper (GILZ) by the glucocorticoid receptor and the PI3-kinase/AKT pathways in multiple myeloma. *J Steroid Biochem Mol Biol* **110**, 244–254.

[61] Mittelstadt PR and Ashwell JD (2001). Inhibition of AP-1 by the glucocorticoid-inducible protein GILZ. *J Biol Chem* **276**, 29603–29610.

[62] Kyle RA and Rajkumar SV (2009). Treatment of multiple myeloma: a comprehensive review. *Clin Lymphoma Myeloma* **9**, 278–288.

[63] Kaufman JL, Nooka A, Vrana M, Gleason C, Heffner LT, and Lonial S (2010). Bortezomib, thalidomide, and dexamethasone as induction therapy for patients with symptomatic multiple myeloma: a retrospective study. *Cancer* **116**, 3143–3151.